Development of Force Compliant in Series Elastic Actuator Systems

Chaiyaporn Silawatchananai and Suppachai Howimanporn
Department of Teacher Training in Mechanical Engineering, Faculty of Technical Education, King Mongkut's University of Technology North Bangkok, Bangkok, Thailand
Email: {chaiyaporn.s, suppachai.h}@fte.kmutnb.ac.th

Piyanun Ruangurai*
Department of Mechanical Engineering Technology, College of Industrial Technology, King Mongkut's University of Technology North Bangkok, Bangkok, Thailand
Email: piyanun.r@cit.kmutnb.ac.th

***Abstract*—This article proposed to develop a prototype and to design the position control with force compliant strategy of reaction force series elastic actuator. The prototype attached an elastic material for absorbing the suddenly exerted force. This work aimed to use as an actuator in human-machine collaborated system which can prevent both indirect/direct damages to the working environment. Two coil springs were installed behind the power transmission of actuator to absorb the reaction force. In this work, the PID and PID-feedforward based position control has been implemented. To evaluate the performance under the load, two test signals: step and ramp signal were used for the reference position of end-effector. The result shows that PID controller providing the RMSE value are 2.12 cm and 3.76 cm, respectively. For PID-feedforward controller, the result shows that the RMSE value of step and ramp input are 10.91 cm and 0.46 cm, respectively. In summary, the PID-feedforward control has the better performance for ramp input under the load. When the end-effectors collides with the obstacle, the impact force is detected by the spring deflection and utilized as the adapted reference position. By applying the force compliant strategy, the result shows that the interaction force can be reduced for 10 times.**

***Index Terms*— series elastic actuator, PID control system, PID-Feedforward control system**

I. INTRODUCTION

Recently the utilization of compliant actuator is increased significantly, especially Series Elastic Actuators (SEA). It has been introduced [1] since 1995 to provide many benefits in force control of robots. The actuators have an elastic element such as a spring attached with the mechanical energy source output, to improve the performance such as low impedance, tolerance to impact loads and passive mechanical energy storage. There are many applications used SEA to improve the performance such as legged actuation systems [2]-[3], in quadriceps robot or human orthotics device [4], compliant joint systems in cooperative robot and advanced mobile robot [5].

Several types of passive elements were integrated in SEA such as electrical clutch, various stiffness springs. Clutchable Series-elastic Actuator (CSEA) was introduced for prosthetic knee [4]. Emre Sariyildiz et.al. designed a variable stiffness SEA by soft and hard springs in series [6]. In robotics research, there are three main configurations [7] of SEA according to the location of elastic element. Force-sensing Series Elastic Actuator (FSEA) has the spring at the end effector which is easy to implement. Transmitted Force-sensing Series Elastic Actuator (TFSEA) has the spring or flexible part at the gear transmission. Lastly Reaction Force-sensing Series Elastic Actuator (RFSEA) locates the spring before the transmission. Thus, each types of SEA have the different consideration for dynamic model and control design.

The University of Texas Series Elastic Actuator or UT-SEA [8] was introduced which is a compact, lightweight actuator by integrating pushrod. A compact planetary geared elastic actuator (cPEA) which consists of planetary gear and torsion spring was proposed in order to reduce space of mechanism [9]. Their work was utilized and in many applications such as Virtual Ground Robot, dynamic dumbbell [10], lower limb rehabilitation [11].

To control the output force or impedance of series elastic Several control schemes mostly based on linear control liked PD or PID controller have been proposed. Tao Q. [12] proposed two PI controllers in cascaded control strategy for FSEA. The PI outer loop is force control that provide the velocity command for inner loop. This work analyzed the stability of the control system and boundaries of control in only simulation. N. Paine [8] proposed the force and position control based on combination of PID, model-based and disturbance observer (DOB) control structure to reduce the force tracking error. Markus G. [13] presented the design of a state-space controller for SEA. Lee D. [14] proposed robust control based on integral sliding mode control with state feedback control with adding DOB.

Manuscript received December 21, 2021; revised March 2, 2022.

doi: 10.18178/ijmerr.11.6.422-428

II. Materials and Methods

A. Dynamical Model

The series elastic actuator for our study as shown in Fig. 1 was developed inspired by [8] which has some highlight features. Firstly, the power of a DC brush motor is transmitted through a pulley and a ball nut, then the ball screw is moved along piston-style housing with support inside. Secondly, the elastic elements were installed around the piston-style housing. Both features are the key compactness of device. Two springs transmit force the actuator housing to the ground base. The springs are supported by the housing part with four ball bearing guide rails which offer a lower friction in translation motion.

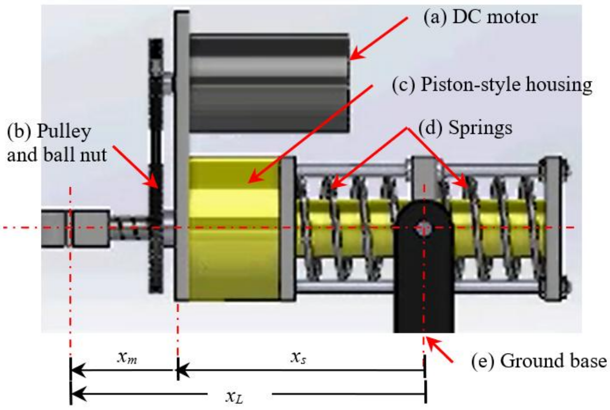

Figure 1. Structure of series elastic actuator.

Refer to Fig. 1, let define the ground base as the reference point of the system, then the position of end effector x_L is the summation of the moving rod position x_m and the spring deflection x_s. Fig. 2 illustrates the unlumped model of SEA that uses a rack and pinion representation as the power transmission. The angular position of DC motor (θ_m) can be converted into the moving rod position by using the transmission ratio (N) as (1). The transmission ratio is depicted as the pulley ratio, the diameter of ball screw and the lead pitch ($N = n\pi D/L$).

$$x_L = N^{-1}\theta - x_s \tag{1}$$

The equation motion of moving rod is expressed in (2) whereas F_{ext} is the exerted force from environment and F_{out} is the reaction force. This reaction force can be sensed by the deviation of spring position x_s which is expressed as mass spring damper model in (3).

$$m_L\ddot{x}_L + b_L\dot{x}_L = F_{out} + F_{ext} \tag{2}$$

$$m_s\ddot{x}_s + b_s\dot{x}_s + K_s x_s = F_{out} \tag{3}$$

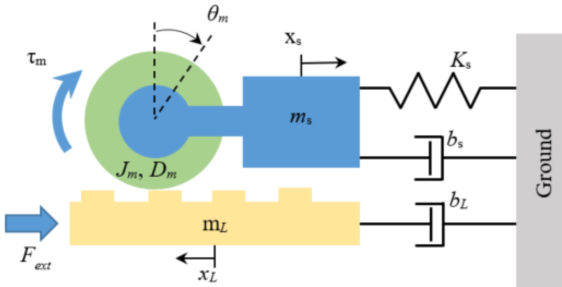

Figure 2. Unlumped dynamic model of RFSEA.

Parameters in the model are defined as follows

m_L is the mass of moving rod.

m_s is the mass of housing part including the motor's frame.

b_L is the viscosity term of moving rod.

b_s is the viscosity term of spring's system.

K_s is the spring constant.

τ_m is the torque generated by motor.

To control the position and force of moving rod, the required torqued generated from DC motor and its transmission needs to be controlled. In this work, the DC motor is driven by H-bride driver circuit, which the duty cycle of pulse with modulation (PWM) signal is proportional to the input voltage. Thus, the electromechanical model also is included so that the SEA dynamical model can be formed as the input voltage, vin. The differential equations of the permanent magnet DC motor in electrical and mechanical terms are expressed in (4) and (5), respectively.

$$R_a I_a + L_a \dot{I}_a + K_b\dot{\theta} = v_{in} \tag{4}$$

$$\begin{aligned} J_m\ddot{\theta} + D_m\dot{\theta} &= \tau_m - N_t^{-1}F_{out} \\ &= K_t I_a - N_t^{-1}F_{out} \end{aligned} \tag{5}$$

where

R_a is the armature resistance.

L_a is the armature inductance.

K_b is E.M.F. voltage constant.

J_m is the inertia of motor's rotor.

D_m is the viscosity term of motor.

K_t is the torque constant.

N_t is the transmission of ball screw.

Equation (1) – (5) can be transformed into Laplace domain for designing the controller. The block diagram of derived dynamic model of SEA system is illustrated in Fig. 3, which is represented as a Multiple–Input-Multiple-Output (MIMO) systems. Two inputs are the input voltage (v_{in}) and the external force (F_{ext}). Two measurable outputs are the motor angle (θ_m) and the spring deflection (x_s).

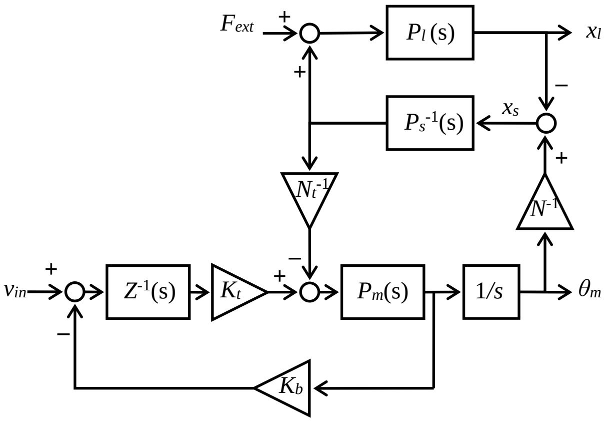

Figure 3. Block diagram of an SEA system including an electromechanical model.

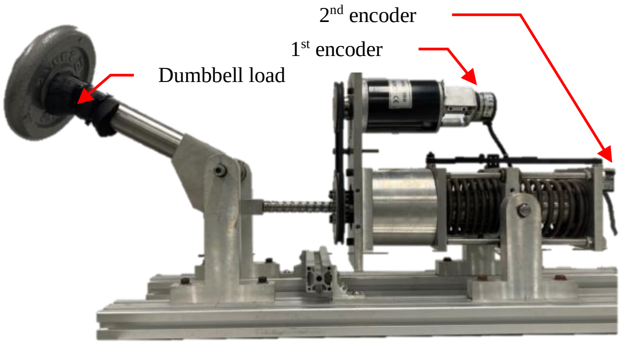

Figure 4. Hardware configuration of SEA.

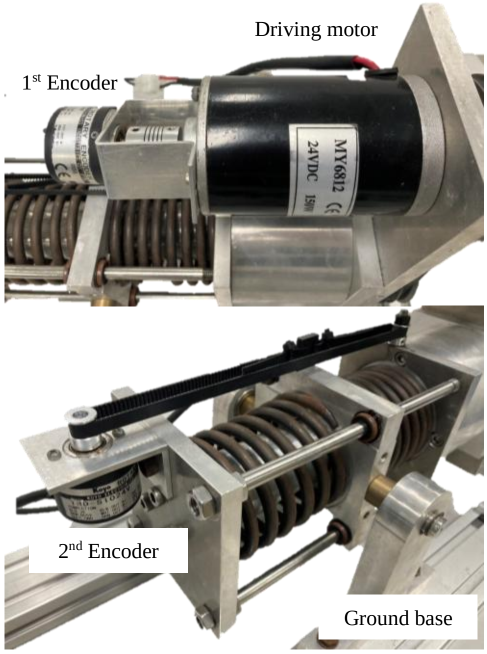

Figure 5. Sensors installed on the SEA.

where

$Z(s) = L_a s + R_a$ represents the electrical impedance.

$P_m^{-1}(s) = J_m s + D_m$ is the motor rotor dynamic.

$P_l^{-1}(s) = m_l s^2 + b_l s$ is the load dynamic.

$P_s^{-1}(s) = m_s s^2 + b_s s + K_s$ is the spring and motor stator dynamics.

The transfer function related between the end-effector position (x_L) among the input voltage (v_{in}) and the external force (F_{ext}).

$$X_L(s) = G_1(s)V_i(s) + G_2(s)F_{ext}(s) \tag{6}$$

B. *Hardware Configuration*

The test bench of SEA is designed, manufactured, and assembled as shown in Fig. 4. The target specification is to provide the maximum output force 50N and the speed of the end-effector is limited at 300mm/s. The power of a 24V 150W DC motor transmits through the 10mm/rev pitch ball screw. The moving rod position is obtained by the 1st encoder attached at the end of motor. The counted pulse signal of the encoder represents the angular position of motor's shaft, the gear ratio related to pulley and the pitch of the screw is used to convert the angular position to the displacement of the end-effector. However, the end-effector position has the reference point at the ground based which the spring deviation occurred when the external force is exerted at the end effector. It is sensed by using the 2nd encoder attached with pulley as shown in Fig. 5, then the displacement is obtained by multiplying the changing in angle with the diameter of pulley (12 mm). Both encoders have the maximum resolution 4,096 counts per round by using quadrature counter.

The dumbbell load is used to provide the external axial force exerting to the moving ball screw, which is varied depended on mass and load position.

The parameters are listed in Table I which the value is obtained by directly measurement as shown in Fig. 6 for the mechanical properties or the identification experiment. These values are substituted into the mathematical model in (6), then the controller gains can be selected.

TABLE I. PARAMETER OF SEA SYSTEM

Component	Parameters	Value	Unit
Mechanical parts	m_s	5.50	Kg
	b_s	270	N s/m
	K_s	4,095	N/m
	m_L	0.52	Kg
	b_L	0.36	N s/m
Driving motor	R_a	0.63	ohm
	L_a	1.73	mH
	K_b	0.092	V s/rad
	K_t	0.092	N m/A
	J_m	5.1×10^{-4}	kg m^2
	D_m	8.0×10^{-4}	N ms/rad
Transmission parts	n	1.4	-
	D	0.016	m
	L	0.010	m/rev

Figure 6. Parameter identifications by directly measurement.

To perform the position control under the external force, a mechanical linkage with movement of dumbbell load generates the axial force to the actuator. As shown in Fig. 7, the moment and the axial force are depending on the arm angle (θ_a) which can be expressed as (7) and (8) by using law of cosine and law of sine.

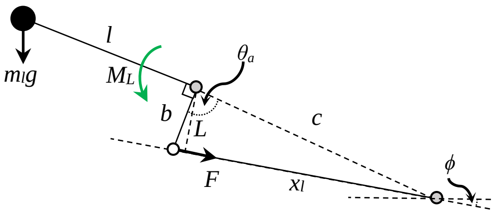

Figure 7. Dimension of a mechanical linkage

$$F = \frac{M_L}{L} = \frac{M_L\sqrt{b^2 + c^2 - 2bc\cos\theta_a}}{bc\sin\theta_a} \tag{7}$$

$$M_L = m_l gl\cos(\theta_a + \phi) \tag{8}$$

Where b is the offset between the link pivot and the pushrod pivot which is obtained from the mechanic part. c is distance between the link pivot and the actuator pivot. l is the center of mass. The dimension used in the experiment are b = 50.0 mm, c = 393.2 mm.

C. System Architecture

In this work, all sensory information and motor command are acquired and sent through NI myRIO board. Personal Computer (PC) installed LabVIEW software which is graphical programming is used to implement control algorithm, adjust the parameters, and observe the system response through graphical user interface (GUI) in real-time. Fig. 8 shows the system architecture of SEA system and the example of LabVIEW program for data acquisition and displaying the response.

D. Controller Design

To improve the performance of the end-effector position control under the load condition, the controller was designed to perform the reference tracking and compensate the external load.

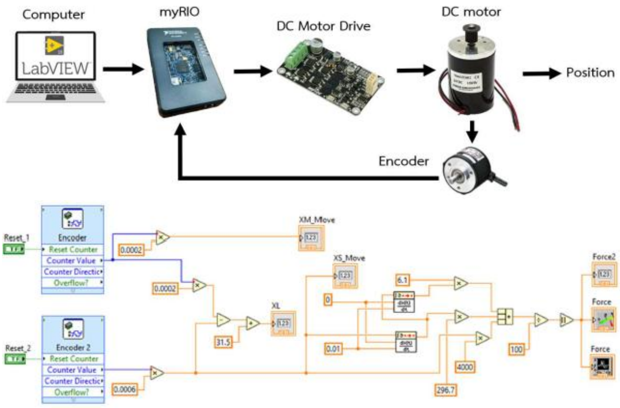

Figure 8. System architecture of SEA system and LabVIEW program.

1) Proportional integral derivative controller

Proportional Integral Derivative (PID) controller is a linear controller which has a simple structure and easy to implement. The output of PID controller is calculated from the summation of proportional integral and derivative value of tracking error expressed in (9). The tracking error is resulting from the changing of reference signal or the external disturbance.

$$u = K_P e + K_I \int edt + K_D \frac{d}{dt}e \tag{9}$$

Three controller gains K_P, K_I and K_D are tuned in order to reduce the tracking error and also changes the system behavior. In practical, the low-pass filter can be added in derivative term to prevent the noise amplification. PID controller with low-pass filter term can be expressed in (10), where τ is the cut-off frequency.

$$\frac{U(s)}{E(s)} = K_P + \frac{K_I}{s} + \frac{K_D s}{\tau s + 1} \tag{10}$$

2) PID plus feed-forward control

PID with feed-forward (PID-FF) controller utilizes feed-forward signal with additional gain to compensate which could be input or disturbance. In this work, the feed-forward term is used as the input compensation, where r is the reference command and K_F is the feed-forward gain.

$$u = K_F r + K_P e + K_I \int edt + K_D \frac{d}{dt}e \tag{11}$$

III. Result and Discussion

A. Position Control under the Load Experiment

This section applied the position control of SEA with dumbbell arm load. Both controllers: PID and PID+FF were implemented in NI myRIO board, then can be selected on the LabVIEW GUI screen. Initially the moving rod is commanded to the zero position, however the measuring end-effector position with the respect to the ground base is at 305 mm. To perform the effect of load in various pose, three set points: 345, 375 and 405 mm are set and changed in either step or ramp. Each step point command was held for 3 seconds. All response data was recorded every 0.01 second.

1) Step response experiment

The result of PID controller performing in step command is shown in Fig. 9. PID controller parameters was tuned at K_P = 0.1, K_I = 0.12 and K_D = 0.0001. Fig. 10 shows the result of PID+FF controller performing in step command. The controller parameters were tuned at K_F = 0.000008, K_P = 0.1, K_I = 0.12 and K_D = 0.0001. By using feed-forward term as input compensation, the response has more overshoot than PID controller's.

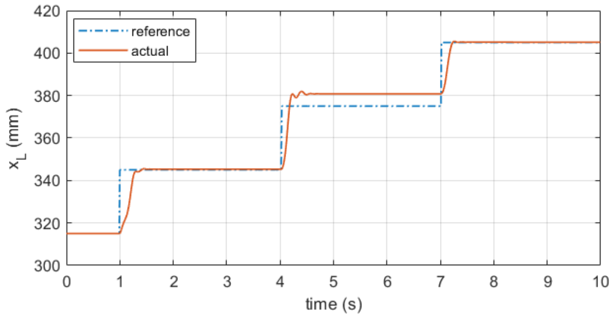

Figure 9. Step response of PID Controller.

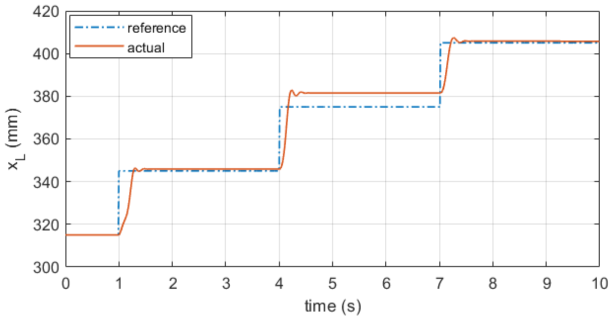

Figure 10. Step response of PID+FF Controller.

The performance of two controllers is compared in Table II. Steady-state error is observed when the response reached in the steady-state region. In the transient response, the settling time and the percentage of overshoot are also indicated to evaluate how fast the response is and how much the response be aggressive, respectively. Notice that the maximum steady-state error occurred at the set point 2 (x_L = 375 mm) for both controllers. The reason is that the dumbbell arm angle was at the straight out at this set point, then the external force is exerted to the actuators in maximum.

TABLE II. PERFORMANCE COMPARISON IN STEP RESPONSE

	Controller	Set point 1	Set point 2	Set point 3
Steady-state Error (mm)	PID	0.29	5.80	0.15
	PID+FF	0.80	6.50	0.80
Settling time (s)	PID	0.59	0.69	0.48
	PID+FF	0.60	0.54	0.59
Overshoot (%)	PID	0.10	1.75	0.12
	PID+FF	0.37	2.10	0.56

For step response, PID controller performs the tracking of step command under the load better than PID+FF in steady-state response and transient response.

2) Ramp response experiment

In this section, the reference position was changed in constant rate to verify the performance of controllers in velocity tracking. During the experiment, each set point was held for 3 second after that changes to the next set point with the rate of change is 50 mm/s. PID controller parameters was tuned at K_P = 0.3, K_I = 0.0004 and K_D = 0.001. The result of PID controller performing in ramp command is shown in Fig. 11.

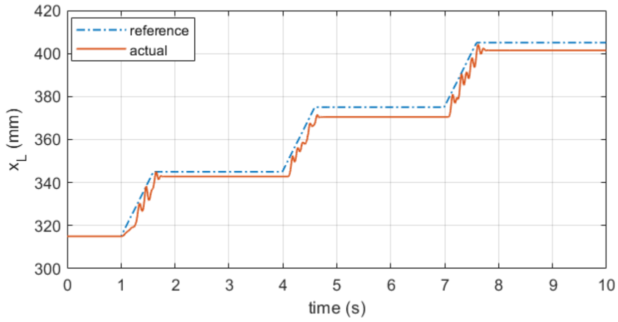

Figure 11. Ramp response of PID Controller.

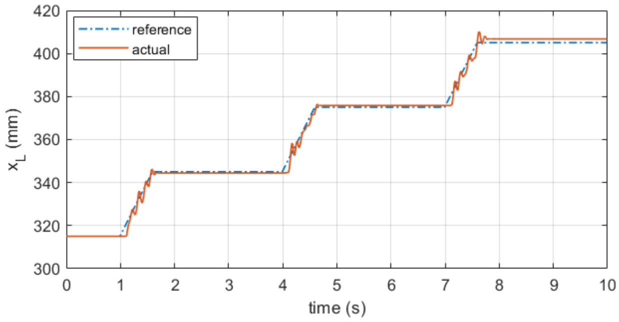

Figure 12. Ramp response of PID+FF Controller.

Fig. 12 shows the result of PID+FF controller performing in step command. The controller parameters were tuned at K_F = 0.004, K_P = 0.3, K_I = 0.0004 and K_D = 0.001.

The tracking performance of two controllers are compared in Table III where the root means square error value is included. For ramp input reference, the RMSE value of PID and PID-feedforward controller are 3.76 cm and 0.46 cm, respectively.

TABLE III. PERFORMANCE COMPARISON IN RAMP RESPONSE

	Controller	Set point 1	Set point 2	Set point 3
Steady-state Error (mm)	PID	0.89	6.50	0.80
	PID+FF	0	0.20	0.17
RMSE (mm)	PID	37.61		
	PID+FF	4.64		

B. Force Control Experiment

In this section, the spring deflection is utilized for collision detection during the tracking position. The reference position is set in maximum and minimum value as 350 mm and 310 mm, respectively, then the target position is changed periodically. In this work, the period of reference position signal is 2 second. The rate of change in set point is constant where the reference position is updated every 0.1 second.

During conducted the experiment, the object was placed as the obstacle as shown in Fig. 13. When the load arm hit the obstacle, the external force exerted on the end-effector was sensed by x_s. There are two cases: with or without force compliant strategy to address the benefit of elastic elements. Fig. 14 shows the time history plot of the end-effector position and the contacting force without force compliant.

There is no obstacle during t = 0 and t = 5 second, then the device keeps the position tracking performance. After 5 second, the collision was occurred and detected with the reference position reached below 325 mm. The result shows that the contacting force is 27.70 N in maximum. In practical, the end-effector cannot move further because of the obstacle. The slide guide can move in the opposite direction with the spring force. This spring force is equal to the output force that act to the environment.

The force compliant strategy is implemented by converting the contacting force to a new reference position. The static gain is multiplied with the contacting force as the new reference position, then adds to the reference position trajectory. When the load arm contacted to the obstacle, the reference position was changed so that the amplitude of contacting force is reduced as shown in Fig. 15, which the peak value is 5.43 N. Even though the position of end-effector cannot reach the original trajectory, the benefit of reduced contacting force is no harmful to surrounding environment.

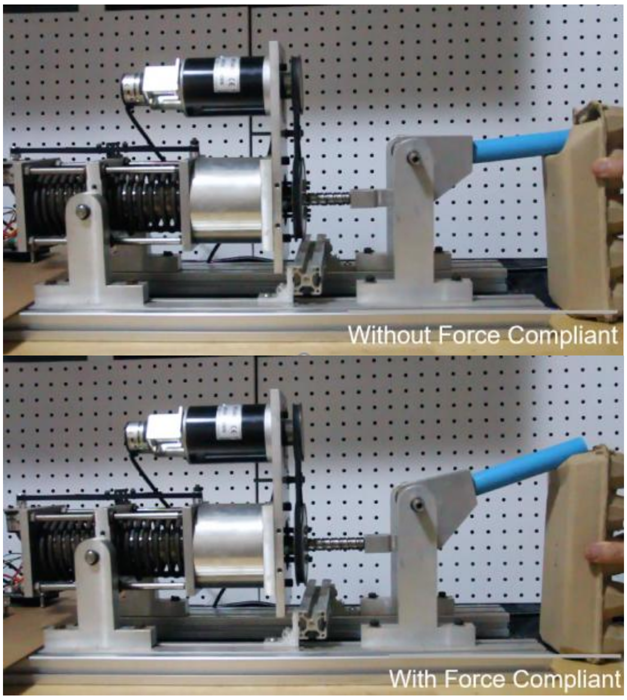

Figure 13. Video shots of force compliant experiment

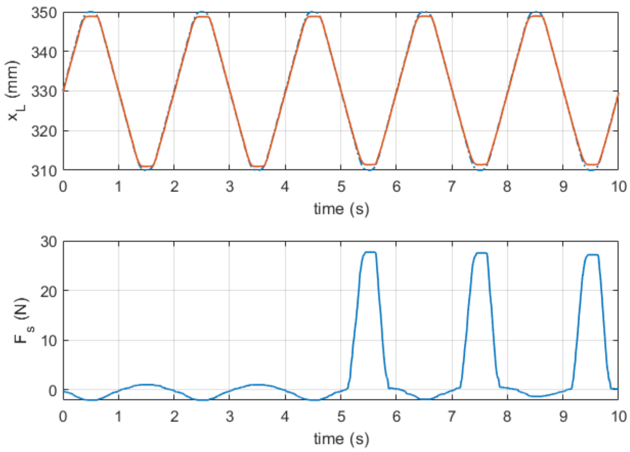

Figure 14. Tracking position without force compliant.

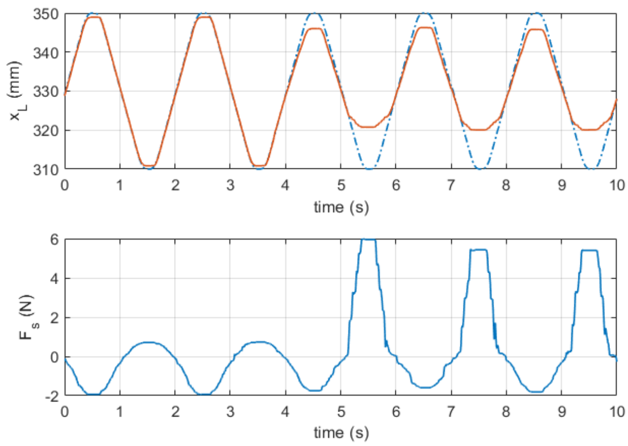

Figure 15. Tracking position result with force compliant.

IV. Conclusion

In this paper, the prototype of SEA has been designed and developed for the position control of end-effector with load compensation and force compliant strategy. This device aims to use as an actuator in human-machine collaborated systems which it can control the interaction force between users or the surrounding environment. The prototype attached an elastic material for absorbing the suddenly exerted force. Two linear controllers: PID and PID with feedforward has been implemented in LabVIEW in order to conduct the experiment.

To evaluate the performance under the load, two test signals: step and ramp signal were used for the reference position of end-effector. The result shows that PID controller providing the RMSE value are 2.12 cm and 3.76 cm, respectively. For PID-feedforward controller, the result shows that the RMSE value of step and ramp input are 10.91 cm and 0.46 cm, respectively. In summary, the PID-feedforward control has the better performance for ramp input under the load. The spring deflection is utilized for collision detection during the tracking position. The adapted reference position based on the interaction force is selected for force compliant strategy. By taking the obstacle at the end-effector's trajectory, the result shows that the interaction force can be decreased for 10 times.

Conflict of Interest

The authors declare no conflict of interest.

Author Contributions

The authors had approved the final version. C. Silawatchananai conducted the research with his under-graduated students who manufactured and assembled the hardware used for the experiments. S. Howimanporn and P. Ruangurai supported the electronic components and guided real-time programming for collection of data. The authors were involved in the drafting of the manuscript and had approved the final version.

Acknowledgment

This research was funded by King Mongkut's University of Technology North Bangkok. Contract no. KMUTNB-64-DRIVE-13.

References

[1] G. A. Pratt and M. M. Williamson, "Series elastic actuators," in *Proc. 1995 IEEE/RSJ International Conference on Intelligent Robots and Systems*, Human Robot Interaction and Cooperative Robots, 1995.

[2] H. Yu, S. Huang, G. Chen, and N. Thakor, "Control design of a novel compliant actuator for rehabilitation robots," *Mechatronics*, vol. 23, no. 8, pp. 1072–1083, December 2013.

[3] J. Vantilt, K. Tanghe, M. Afschrift, *et al*. "Model-based control for exoskeletons with series elastic actuators evaluated on sit-to-stand movements," *J NeuroEngineering Rehabil*, vol. 16, no. 65 2019.

[4] E. J. Rouse, L. M. Mooney, and H. M. Herr, "Clutchable series-elastic actuator: Implications for prosthetic knee design," *The international Journal of Robotics Research*, vol.33, no. 13, p. 1611-1625, November 2014.

[5] A. Kakogawa and S. Ma, "An In-pipe inspection module with an omnidirectional bent-pipe self-adaptation mechanism using a joint torque control," in *Proc. 2019 IEEE/RSJ International Conference on Intelligent Robots and Systems (IROS)*, 2019, pp. 4347-4352.

[6] E. Sariyildiz, G. Chen, and H. Yu, "Robust position control of a novel series elastic actuator via disturbance observer," in *Proc. 2015 IEEE/RSJ International Conference on Intelligent Robots and Systems (IROS)*, 2015, pp. 5423–5428.

[7] C. Lee, S. Kwak, J. Kwak, and S. Oh, "Generalization of series elastic actuator configurations and dynamic behavior comparison," *Actuator*, vol. 6, no. 26, pp. 1–26, 2017.

[8] N. Paine, S. Oh, and L. Sentis, "Design and control considerations for high-performance series elastic actuators," *IEEE/ASME Trans. Mechatronics*, vol. 19, no. 3, pp. 1080–1091, June 2014.

[9] C. Lee and S. Oh, "Configuration and performance analysis of a compact planetary geared Elastic Actuator," in *IECON Proc. (Industrial Electronics Conference)*, 2016, October 2016, pp. 6391–6396.

[10] C. Lee and S. Oh, "Dynamic dumbbell - novel muscle training robot with programmable exercise load," in *Proc. IEEE International Conference on Intelligent Robots and Systems*, 2018, no. 10080547, pp. 7648–7653.

[11] C. Lee, J. Kim, S. Kim, and S. Oh, "Human force observation and assistance for lower limb rehabilitation using wire-driven series elastic actuator," *Mechatronics*, vol. 55, 2018, pp. 13–26.

[12] T. Qiao and S. Bi, "Cascaded control of compliant actuator in friendly robotics," *UPB Scientific Bulletin, Series D: Mechanical Engineering*, vol. 75, no. 1, pp. 73–88, 2013.

[13] M. Grun, R. Muller, and U. Konigorski, "Model based control of series elastic actuators," in *Proc. IEEE RAS EMBS Int. Conf. Biomed. Robot. Biomechatronics*, no. 3, pp. 538–543, 2012.

[14] D. Lee, S. Park, and G. Kwak, "Robust control of series elastic actuator using ISMC and DOB," *International Journal of Mechanical Engineering and Robotics Research*, vol. 9, no. 1, pp. 25–29, 2020.

Chaiyaporn Silawatchananai graduated bachelor's degree in engineering major in electrical engineering from Sirindhorn International Institute of Technology, Thammasat University. He was received master's and doctoral degree in mechatronic engineering from Asian Institute of Technology. Currently, he has been an Assistant Professor with major of mechatronics engineering, department of teacher training in mechanical engineering, faculty of technical education, King Mongkut's University of Technology North Bangkok. His research interests in the field of robotics, automation, model-based and embedded control systems.

Suppachai Howimanporn was born in Bangkok, Thailand in 1975. He received B.Eng. in electrical engineering, M.Eng. in control engineering from King Mongkut's Institute of Technology Ladkrabang, Thailand in 1999 and 2004, and D.Eng. degree in mechatronics at School of Engineering and Technology, Asian Institute of Technology, Thailand in 2014. From 2005 to 2014, he was a lecturer in Department of Electrical Engineering, Faculty of Industrial education, Rajamangala University of Technology Phra Nakhon Bangkok, Thailand. Since 2015, he has been an Assistant Professor with Major of Mechatronics Engineering, Department of Teacher Training in Mechanical engineering, Faculty of Technical Education, King Mongkut's University of Technology North Bangkok, Thailand. His research interests include control systems, robotics, automation and mechatronics.

Piyanun Ruangurai graduated bachelor's degree in engineering major in electronic engineering from King Mongkut's Institute of Technology Ladkrabang. She was received master's degree in microelectronics and embedded systems engineering from Asian Institute of Technology. She is the lecturer at College of Industrial Technology, King Mongkut's University of Technology North Bangkok. Her research interests in the field of image processing, machine visions and embedded systems.